Plant Molecular Biology (2023) 112:309–323
https://doi.org/10.1007/s11103-023-01365-1

Mucilage secretion by aerial roots in sorghum (*Sorghum bicolor*): sugar profile, genetic diversity, GWAS and transcriptomic analysis

Si Xu[1,2] · Xiu-Qing Li[3,4] · Hong Guo[1,2] · Xiao-Yuan Wu[1] · Ning Wang[1] · Zhi-Quan Liu[1,5] · Huai-Qing Hao[1,2] · Hai-Chun Jing[1,2,5]

Received: 4 January 2023 / Accepted: 3 June 2023 / Published online: 28 June 2023

Abstract

Aerial root mucilage can enhance nitrogen fixation by providing sugar and low oxygen environment to the rhizosphere microbiome in Sierra Mixe maize. Aerial root mucilage has long been documented in sorghum (*Sorghum bicolor*), but little is known about the biological significance, genotypic variation, and genetic regulation of this biological process. In the present study, we found that a large variation of mucilage secretion capacity existed in a sorghum panel consisting of 146 accessions. Mucilage secretion occurred primarily in young aerial roots under adequately humid conditions but decreased or stopped in mature long aerial roots or under dry conditions. The main components of the mucilage-soluble were glucose and fructose, as revealed by sugar profiling of cultivated and wild sorghum. The mucilage secretion capacity of landrace grain sorghum was significantly higher than that of wild sorghum. Transcriptome analysis revealed that 1844 genes were upregulated and 2617 genes were downregulated in mucilage secreting roots. Amongst these 4461 differentially expressed genes, 82 genes belonged to glycosyltransferases and glucuronidation pathways. *Sobic.010G120200*, encoding a UDP-glycosyltransferase, was identified by both GWAS and transcriptome analysis as a candidate gene, which may be involved in the regulation of mucilage secretion in sorghum through a negative regulatory mechanism.

Key message

Sorghum accessions showed considerable genotypic variation in mucilage secretion. Both GWAS and transcriptome analyses suggested the involvement of a UDP-glycosyltransferase gene (*Sobic.010G120200*) and the glucuronidation pathway in mucilage secretion in sorghum.

Keywords Mucilage secretion · Aerial root development and exudates · Sorghum (*Sorghum bicolor*) · Transcriptome · GWAS

Background

Plants release various exudates from the aboveground and underground parts into the surrounding environment in the form of solid, liquid, or gaseous substances, of which the liquid ones are called mucilage (Galloway et al. 2020; Sasse et al. 2018). Almost all clades of angiosperms can secrete exudates, which play specific roles in plant growth and development, nutrient absorption, and stress resistance (Brown et al. 2017; Galloway et al. 2020; Sasse et al. 2018). Plant organs which can generate exudates mainly include adventitious roots, abnormal leaves, and seed coats. The adventitious roots of climbing fig (*Ficus pumila*) and English ivy (*Hedera helix*) can be firmly fixed on the vertical surface through the chemical adhesion of

✉ Huai-Qing Hao
hqhao@ibcas.ac.cn

1 Key Laboratory of Plant Resources, Institute of Botany, Chinese Academy of Science, Beijing 100093, China

2 University of Chinese Academy of Sciences, Beijing 100049, China

3 Fredericton Research and Development Centre, Agriculture and Agri-Food Canada, Fredericton, NB E3B 4Z7, Canada

4 Canada Forage International Inc., Fredericton, NB, Canada

5 Engineering Laboratory for Grass-Based Livestock Husbandry, Institute of Botany, Chinese Academy of Sciences, Beijing 100093, China

exudates (Groot et al. 2003; Melzer et al. 2010). Carnivorous plants such as *Nepenthes sp.*, *Drosera peltata* and *Pinguicula vulgaris* (Adlassnig et al. 2010; Gaume and Forterre 2007; Huang et al. 2015), trap and decompose animals through exudates to improve the supply of minerals, nitrogen and phosphorus nutrients. The exudates produced by *Arabidopsis thaliana* seed coat epidermal cells are essential for seed viability and germination, which have water retention ability and increase the water utilisation rate of seeds and make them less susceptible to short-term drought (Haughn and Western 2012; Huang et al. 2004).

Root exudates refer to various substances secreted or released into the environment by different parts of the root system, and have been extensively examined in the underground root systems. The exudates from the underground roots mainly include sugars, amino acids, fatty acids, nucleotides, proteins and enzymes (Badri and Vivanco 2009; Baetz and Martinoia 2014; Bais et al. 2006; Czarnes et al. 2000a; Narasimhan et al. 2003; Read et al. 2003; Read and Gregory 1997), which can potentially attract beneficial microorganisms and affect the enrichment of the rhizosphere microbiota, thereby enhancing the ability of plants to adapt to the environment (Bulgarelli et al. 2013; Sigida et al. 2013; Zhalnina et al. 2018). Root exudates can also maintain the soil moisture in the rhizosphere and stabilise the structure of rhizosphere soil affected by the adsorption (Carminati 2012; Carminati et al. 2016; Czarnes et al. 2000b). In contrast to the wealthy information on the exudates of underground roots, little is known about exudates from aerial roots on the aboveground part of plants. Until 2018, mucilage secretion biological significance was documented in the aerial roots of Sierra Mixe maize (Van Deynze et al. 2018). It has been proven that mucilage is a key component for maize to cooperate with nitrogen-fixing microorganisms to perform efficient nitrogen fixation (Bennett et al. 2020; Van Deynze et al. 2018).

The molecular basis of mucilage secretion has been mainly investigated in the special secretory cells of *Arabidopsis* seed coat. The mucilage of most plant exudates contains adhesive components mainly consisting of polysaccharides, which are either formed by monosaccharide cytosolic synthesis or formed by glycosyl-transferase enzymes within Golgi apparatus (Galloway et al. 2020; Sechet et al. 2018; Voiniciuc et al. 2018b). In addition, some proteins and enzymes such as galaturonosyl transferase (GAUT), cellulose synthase-like (CSL), and rhamnose biosynthesis (RHM), are packaged into vesicles and then exported to the plasma membrane for mucilage secretion (Arsovski et al. 2010; Galloway et al. 2020; Tsai et al. 2017). However, whether similar adhesive components and cellular enzymes could be found in the mucilage of aerial roots remains unknown.

Sorghum (*Sorghum bicolor*) has strong tolerance to abiotic stresses including drought, waterlogging, salinity-alkalinity, and low fertility, and can produce a crop under low-input farming systems (Zhu et al. 2021), which allows it to predominantly grow in sub-Saharan Africa and South Asia as a staple food supporting about 500 million people (Mace et al. 2013) and is globally used for the production of sugar compounds, silage, biomass energy and bioethanol (Brenton et al. 2016; Rooney et al. 2007; Zheng et al. 2011). Sorghum is a crop widely documented with aerial root growth on the shoot nodes, but mucilage secretion by aerial roots was only reported in the proceedings of a conference on cereal nitrogen fixation held in India in 1984 (Wani 1986), and the presence of *Azospirillum brasilense* in the secreted mucilage of the aerial roots implied that mucilage is potentially related to nitrogen fixation. However, the phenomenon of mucilage secretion by aerial roots in sorghum has not been examined in detail, and the mechanisms and genetic diversity of mucilage secretion at the population level are not clear.

In this study, we analysed the effects of aerial root growth and air moisture on mucilage secretion and examined the cytological, metabolic, and transcriptomic basis associated with mucilage secretion in sorghum. The genetic diversity of mucilage secretion was also examined at the population level using a panel of 146 sorghum accessions consisting of wild, landrace, and improved lines. Our study demonstrated that mucilage secretion by aerial root may be an important biological trait with potential implications for sorghum growth and agricultural production.

Results

Mucilage secretion from sorghum aerial roots under different air and soil moisture conditions

In field experiments examining the variation in agronomically important traits, we accidentally noticed the mucilage secretion by aerial roots on rainy days in a number of sorghum accessions. We then assumed that mucilage secretion may have important implications in sorghum growth and production and carried out detailed observations using sorghum Accession 59 which is characterized by prominent growth of aerial roots.

Plants of Accession 59, with large shoots and abundant aerial roots on the nodes, were grown from April to October until the onset of the cold dew in the field, or planted in pots in the greenhouse (Fig. 1a, b). On sunny days with low humidity in the field or without water spraying in the glasshouse, no mucilage secretion could be observed (Fig. 1c). However, a large amount of mucilage can be secreted onto the surface of the aerial roots under high humidity or rainy conditions in summer (Fig. 1d). We further tested the effects

Fig. 1 Aaerial roots and mucilage secretion in sorghum and maize under field and glasshouse conditions. Plants of sorghum Accession 59 were grown in the field (**a**) and the glasshouse (**b**) for 4 months, respectively. There was no mucilage secretion from the aerial roots under sunny conditions in the field or without water spray, as shown by the aerial roots of Accession 59 (**c**) grown in the field for 4 months. Mucilage was observed on the aerial roots of 4-month-old Accession 59 grown for 4 months after rain in the field (**d**), or following continuous water spraying for 24 h in the glasshouse (**e**). Mucilage secretion on the aerial roots of a wild sorghum Accession SL35 grown for 4 months and a maize line B73 grown for 2.5 months after rain in the field (**f**, **h**) or following continuous water spraying in the glasshouse (**g**, **i**). Bars represent 0.5 m in **a** and **b**, 5 cm in **c**, and 1 cm in **d**–**i**, respectively. At least three plants for each line were investigated

of surface humidity on mucilage secretion in the greenhouse by continuously spraying the aerial roots with water. Large amounts of mucilage can be reproducibly observed following overnight water spraying (Fig. 1e). Hence, mucilage secretion was prominently influenced by the surface moisture of the aerial roots. Mucilage secretion was further verified with a wild sorghum Accession SL35 both in the field and glasshouse (Fig. 1f, g). As an analogy, we tested the mucilage secretion from the aerial roots of maize inbred line B73 under the same experimental settings, and found that the results could be reproducibly observed once sufficient surface moisture was attained, either after rain or following continuous water spraying (Fig. 1h, i). Taken together, these results demonstrated that mucilage secretion was a common biological trait in both sorghum and maize with aerial roots and was strongly influenced by the air moisture conditions.

The relationship between growth stage and mucilage secretion capacity of the aerial roots

To accurately measure the capacity of aerial root mucilage secretion, we developed an assay for the mucilage secretion capacity. The specific process was as follows: first, the required length of the aerial root segment starting from the root tip was measured and then cut; second, the aerial root segment was put into a 10-mL centrifuge tube with 5 mL sterilized ddH_2O weighted and placed at the room temperature (~ 25 °C) for 48 h; third, an absorbent paper was used to absorb the water in the tube; fourth, the aerial root with mucilage and tube were weighed together. The mucilage weight was calculated by subtracting the weight of the aerial root and empty tube from the value of step fourth, and the quantification of mucilage secretion capacity was the ratio of mucilage weight to aerial roots weight (Fig. 2a). By recording the length of aerial roots formation from day 1 to day 30, we found that aerial root length increased with extension of growth time. Aerial root length reached its maximum after 20 days and remained unchanged (Fig. 2b). Therefore, length can be used as an indicator for identifying aerial root developmental stages. Based on the above finding, we investigated the relationship between different root lengths and mucilage weight. The mucilage weight reached the highest when the root length is 1 cm and remained quite stable during the period of root length from 1.5 cm to 2.5 cm. Our results showed that the mucilage weight was related to the developmental stage of aerial root (Figs. 2c, S1).

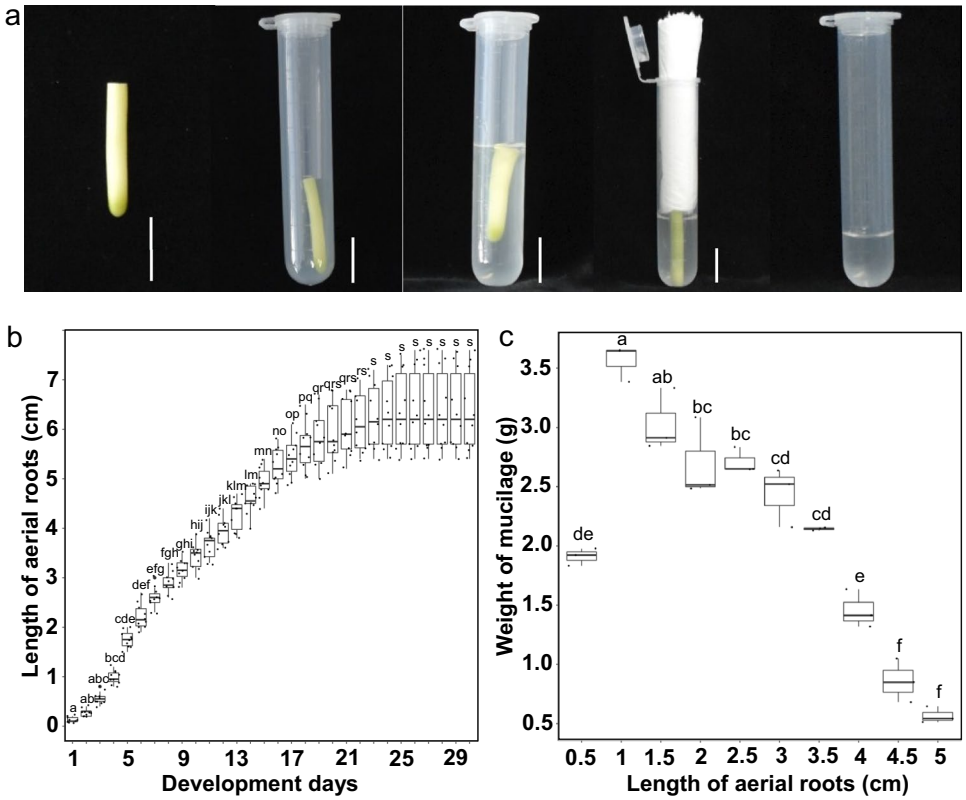

Fig. 2 The relationship between mucilage secretion and the growth and development of aerial roots. **a** Representative micrographs show the experimental procedures for quantification of the amount of mucilage secretion from the aerial roots. Aerial roots of 0.5–5 cm in length were excised from the nodes and collected into a 10-mL Eppendorf tube and weighed, then 5 mL deionised water was added to immerse the aerial root. After 48 h incubation at ambient room temperature, the excessive water was removed from the tube with absorbent paper. The weight of the aerial root together with the secreted mucilage was quantified. The mucilage weight was calculated through the weight of the aerial root, mucilage and empty tube minus the weight of the root and empty tube. **b** The length of aerial roots developed within 30 days. Five biological replicates were selected, and two aerial roots were taken from each biological replicate for measurement, the values are means ± standard deviation (SD) with five biological replicates and two technical replicates in each biological replicate**,** letters indicate a significant difference ($P < 0.05$) using Kruskal test. **c** The weight of mucilage at different aerial root lengths, the values are means ± standard deviation (SD) with three biological replicates, letters indicate a significant difference ($P < 0.05$) using Tukey–Kramer test. Bar represents 1 cm

Microscopic observation and analysis of the sugar profile of mucilage

Using cryo-scanning electron microscopy, the sublimation of water in mucilage and the structure of the residual dry mucilage were visualized. The dry mucilage of Accession 59 and SL36 had a three-dimensional porous network structure possessing interconnected nano to micron-sized pores (Fig. 3a, b). This kind of structure provides space for water, which partly explains the clear, gelatinous state of mucilage that contacts the water. Furthermore, High Performance Liquid Chromatography (HPLC) was used to quantitatively analyze the soluble sugars (fructose, arabinose, galactose, glucose, xylose, mannose, fructose, ribose, galacturonic acid, glucuronic acid, and sucrose) in mucilage. The sugar profile of mucilage from cultivated sorghum (Accession 59) and wild sorghum (Accession SL36) showed that the mucilage was mainly composed of glucose and fructose (Fig. 3c, d). The glucose content was 15.69 µg/mg and the fructose content was 10.33 µg/mg in Accession 59, while the glucose content was 33.68 µg/mg and fructose content was 17.13 µg/mg in Accession SL36. Except for glucose and fructose, the content of other sugars was all less than 0.2 µg/mg in both sorghum lines.

Transcriptomic analysis of mucilage-secreting and non-mucilage-secreting aerial roots

Figure 4a shows the aerial roots used in RNA sequencing: 5-day-old aerial roots with mucilage after rain (when extra rainwater was gone), and the non-secreting roots also at the 5-day age under dry conditions (served as a control). Comparative transcriptomic analysis revealed 4461 differentially expressed genes (DEGs) between mucilage secreting roots and non-secreting roots. Amongst all the DEGs, 1844 genes were upregulated and 2617 genes were downregulated in secreting roots. GO analysis revealed that DEGs were enriched for GO terms related to glycosyltransferase and glucuronidation including quercetin 7-O-glucosyltransferase, quercetin 3-O-glucosyltransferase activity, UDP-glucosyltransferase, glucuronate metabolic process, cellular glucuronidation, flavonoid glucuronidation, uronic acid metabolic process, and glucosyltransferase. And these 8 categories contained 82 genes according to the GO annotation (Fig. 4b, Table S1). Amongst the 82 genes in the heatmap, 32 genes were upregulated and 50 genes were downregulated in mucilage-secreting roots (Fig. 4c, Table S2). qRT-PCR of six downregulated and four upregulated genes randomly selected showed the same results as RNA-Seq results in different aerial roots (Figs. S3a, S3b). Amongst the 82 genes, six genes were involved in known metabolic pathways (Fig. 4d): *Sobic.010G072300*, encoding a sucrose synthase involved in the synthesis of UDP-glucose; *Sobic.002G116000*,

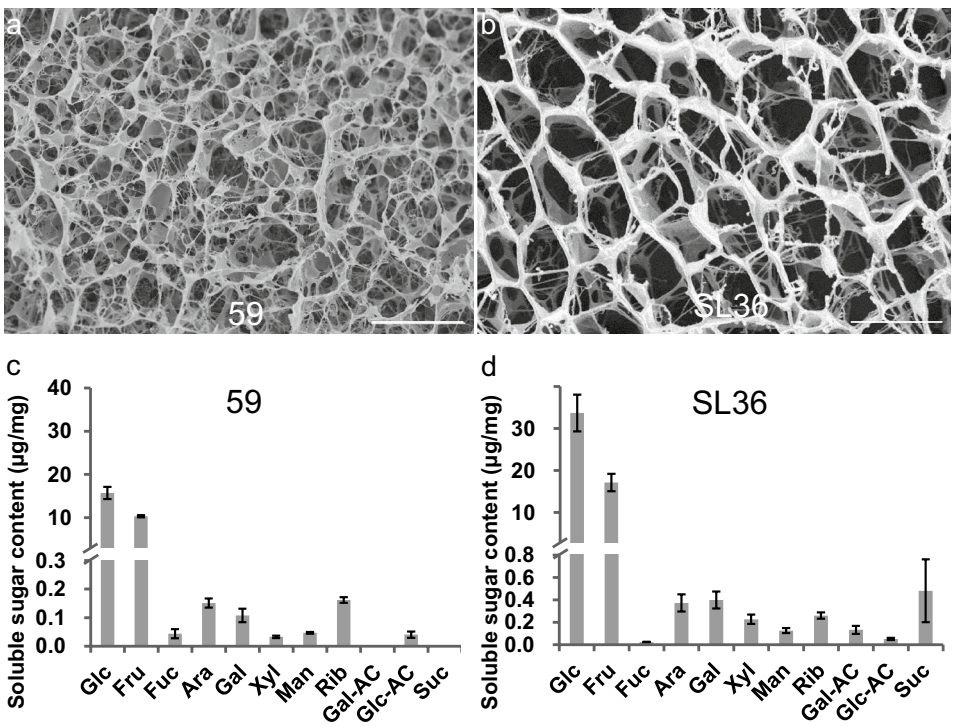

Fig. 3 Mucilage microstructure and the content of soluble sugar. The microscopic state of mucilage secretion after rain was observed by cryo-electron microscopy secreted by Accession 59 (**a**) and SL36 (**b**). The content of soluble sugar in mucilage secreted by aerial roots of Accession 59 (**c**) and SL36 (**d**), the values are means ± standard deviation (SD) with three technical replicates. Bars represent 5 µm in **a** and **b**

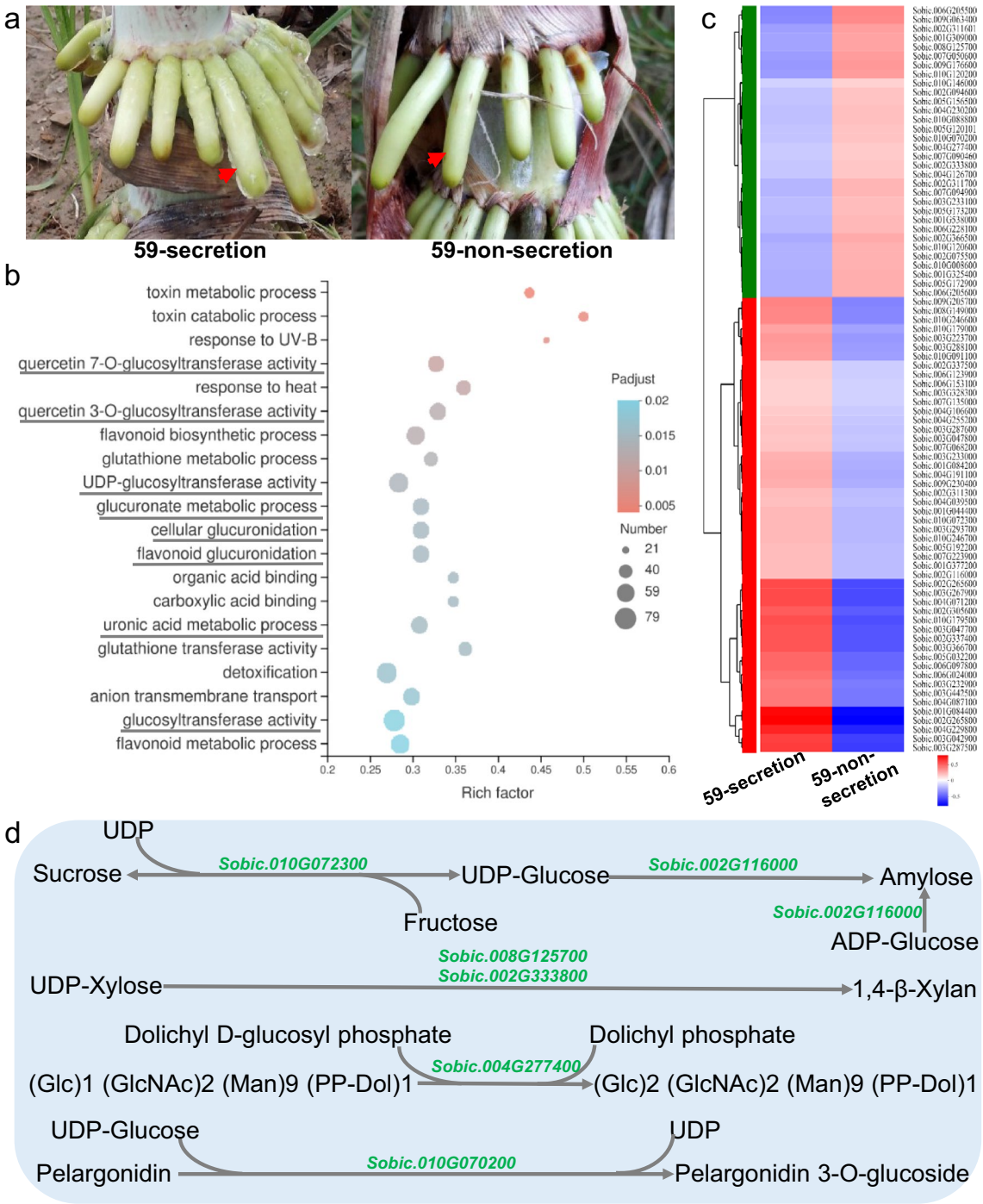

Fig. 4 Gene expression profiles associated with mucilage secretion under transcriptome analysis. **a** The aerial root tissues (59-secretion and 59-non-secretion) used for transcriptome sequencing, show the phenotypic differences in the mucilage secretion of aerial roots under different weather conditions. **b** 59-secretion vs 59-non-secretion GO enrichment analysis results. The vertical axis represents the GO category, and the horizontal axis represents the rich factor. The larger the rich factor, the greater the degree of enrichment. The size of the dot indicates the number of genes in the GO category, and the color of the dot corresponds to different ranges of adjusted *P* value. GO categories related to glycosyltransferase were indicated with underlines. **c** Expression levels of DEGs involved in glycosyltransferase related terms. **d** Detailed known metabolism pathway involved in GO categories related to glycosyltransferases using KEGG KOs-numbers from Interactive Pathways Explorer (http://pathways.embl.de)

encoding a granule-bound starch synthase involved in the synthesis of amylose; *Sobic.008G125700* encoding a cellulose synthase-like protein; *Sobic.002G333800* encoding a mixed-linked glucan synthase involved in the synthesis of 1,4-β-xylan that belong to the pathway amino sugar and nucleotide sugar metabolism; *Sobic.004G277400*, involved in the synthesis of (Glc)2(GlcNAc)2(Man)9(PP-Dol)1 which participated in N-glycan precursor biosynthesis; *Sobic.010G070200* encoding an anthocyanidin 3-O-glucosyltransferase involved in the synthesis of pelargonidin 3-O-glucoside that belong to the anthocyanin biosynthetic pathway. Amongst these six genes, *Sobic.010G072300* and *Sobic.002G116000* were downregulated, and *Sobic.008G125700*, *Sobic.002G333800*, *Sobic.004G277400* and *Sobic.010G070200* were upregulated in mucilage-secreting aerial roots compared to the non-mucilage-secreting aerial roots (Table S2).

Large variation in mucilage secretion capacity and correlation with a stay-green degree in sorghum accessions

To explore the change in mucilage secretion by aerial roots during the domestication and genetic improvement of sorghum, we collected the mucilage secretion capacity data of 146 sorghum accessions (Fig. 5a), including 12 wild sorghum accessions (Wild), 28 landrace grain sorghum accessions (LG), 28 improved grain sorghum accessions (IG) and 78 improved sweet grain sorghum accessions (IS). Statistical analysis showed that the mucilage secretion capacity of the LG subgroup was significantly higher than that of the wild subgroup (Fig. 5b), while there was no significant difference amongst the other subgroups.

We then investigated the correlation between mucilage secretion and agronomic traits. Mucilage secretion capacity

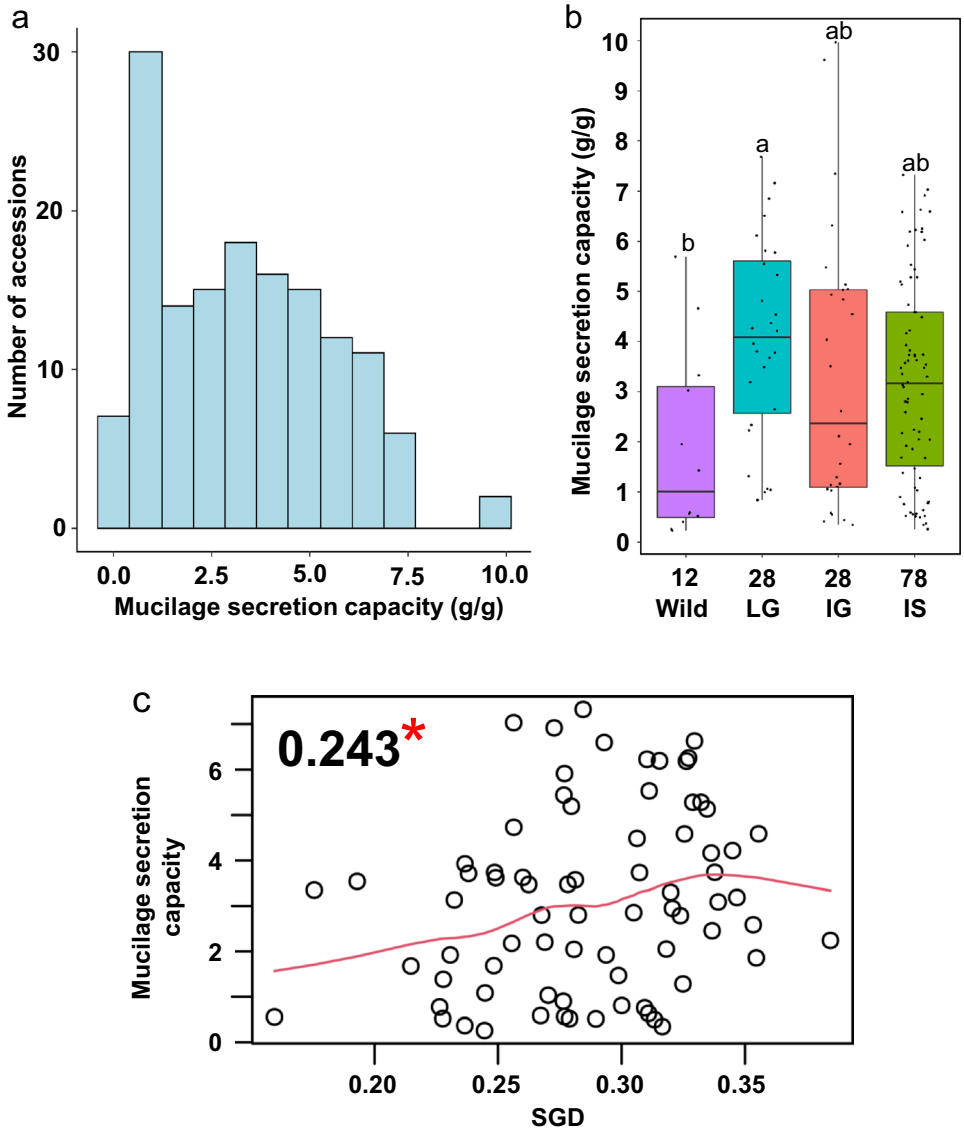

Fig. 5 Variation of mucilage secretion capacity in sorghum. **a** The histogram shows the frequency distribution of mucilage secretion capacity of 146 sorghum accessions. **b** The boxplot shows the mucilage secretion capacity in wild sorghum (Wild), Landrace grain sorghum (LG), improved grain sorghum (IG), improved sweet sorghum (IS). In box plots, center values are averages, lines indicate variability outside the upper and lower quartiles, letters indicate a significant difference ($P < 0.05$) using Tukey–Kramer test. **c** Pearson's correlations amongst stay-green degree (SGD) and mucilage secretion capacity of 75 accessions in IS subgroups. The red line through the scatter plot represents the line of the best fit. The correlation significance level is $*P < 0.05$

was correlated with stay-green degree (SGD) in IS subgroup (Fig. 5c, Table S4). However, when all 126 accessions (20 accessions with missing data were removed from 146 accessions) were analyzed together, there was no correlation between mucilage secretion capacity and the SGD traits. No correlation was detected between mucilage secretion capacity and other traits, including hundred-grain weight (HGW), plant height (PH), stem weight (SW), brix (SB), number of internode (IN), panicle weight (PW) amongst total 54 accessions (92 accessions with missing data were removed from 146 accessions) (Tables S4, S5), regardless in the sweet sorghum group or the total 126 accession population. Therefore, mucilage secretion capacity was correlated only with SGD in improved sweet sorghum.

Association mapping and identification of candidate genes

To dissect the genetic basis underlying the natural variation of mucilage secretion in sorghum, we tested the association of mucilage secretion capacity. From our previously published data (Wu et al. 2022), 4,505,122 SNPs for the 146 accessions in this study were extracted to conduct a genome-wide association study (GWAS) (Fig. 6a), and the quantile–quantile plot was shown in Fig. S4. We further analyzed the potential candidate genes residing within the Significantly Associate Loci (SAL) obtained from the GWAS results (Fig. 6b). Significant difference ($P = 0.045$) in mucilage secretion capacity between accessions with two alleles (T-allele and C-allele) was detected (Fig. 6c), suggesting its important role in regulating mucilage secretion capacity in sorghum. Amongst the 27 genes found in the SAL (Table S7), only one candidate gene, *Sobic.010G120200*, is located in the region of 50 kb upstream and 50 kb downstream around the most significant SNP Chr10:13734925. *Sobic.010G120200* (~ 27.8 kb from the significant SNP Chr10: 13734925) was predicted to encode a UDP-glycosyltransferase and it was in high LD (Linkage Disequilibrium) ($r^2 = 0.93$) with the SNP Chr10:13734925 (Fig. 6d). The haplotypes analysis of *Sobic.010G120200* in 30 sorghum accessions showed that 15 accessions with the T-allele, had high mucilage secretion capacity, and other 15 accessions with the C-allele had low mucilage secretion capacity. We selected 14 significant tag SNPs with a significant difference ($P < 0.05$) of mucilage secretion capacity from a total of 17 SNPs (Tables S8) and constructed four major haplotypes. Hap1 belongs to T-allele and Hap2-Hap4 belong to C-allele (Fig. 7a). Statistically, mucilage secretion capacity of Hap1 accessions was significantly higher than that of Hap2, Hap3, and Hap4 accessions, while there were no significant differences amongst Hap2, Hap3, and Hap4 accessions (Fig. 7b), accounting for phenotypic variance in the two alleles. We further conducted qRT-PCR of *Sobic.010G120200* in the aerial roots of three T-allele accessions (59, WSC99, 197) with higher mucilage secretion capacity and three C-allele accessions (30, J150, 137) with lower mucilage secretion capacity after 12-h water immersion. The results showed that the expression level of *Sobic.010G120200* in the six accessions was significantly decreased after 12-h water immersion. In addition, *Sobic.010G120200* expressed significantly lower in the T-allele accessions than in the C-allele accessions at 0-h and 12-h of water immersion, respectively (Fig. 7c).

Discussion

It was reported that mucilage in Sierra Mixe maize is the key factor for efficient nitrogen fixation, providing a carbon source and a low-oxygen environment that can be utilized by endogenous or recruited microorganisms from the environment (Bennett et al. 2020; Van Deynze et al. 2018). Meanwhile, mucilage secretion existed in a wild relative of maize (*Z. mays ssp. Mexicana*) is much less than cultivated Sierra Mixe maize (*Z. mays* S. Mixe) (Van Deynze et al. 2018). In the present study, we found that it is common for sorghum to grow a large number of aerial roots, and mucilage could be secreted under rainfall, water spray, and water immersion (Figs. 1, 2). Although mucilage secretion in sorghum is common both in wild and cultivated lines, the mucilage secretion capacity of different sorghum accessions varies greatly (Fig. 5). Based on mucilage secreted from the aerial roots contributes to nitrogen fixation with diazotrophic bacteria in Sierra Mixe maize (Bennett et al. 2020; Higdon et al. 2020; Van Deynze et al. 2018), and the landrace grain sorghums have a higher mucilage secretion capacity than the wild sorghums (Fig. 5), which may contribute to secrete more mucilage for microorganisms utilization and nitrogen fixation, leading to the positive selection of mucilage secretion trait to a certain extent. In Sierra Mixe maize, sugar-rich mucilage facilitated the growth of a nitrogen-fixing microbiome, and atmospheric nitrogen fixation contributed 29%–82% of the nitrogen nutrition in plants (Van Deynze et al. 2018). And the supply of nitrogen can delay leaf senescence and enhance the stay-green degree which maintains a higher photosynthetic rate (Borrell et al. 2001; Li et al. 2012; Van Oosterom et al. 2010). As mucilage secreted from aerial roots is common, we suspected that aerial roots and mucilage may also be involved in nitrogen fixation in sorghum, and nitrogen contributes to the stay-green degree of leaves because both maize and sorghum are C_4 plants with similar aerial roots and mucilage secretion. In addition, the detection of *Azospirillum brasilense* has also been reported in sorghum (Wani 1986). This potential association with nitrogen fixation may provide support for the correlation between the

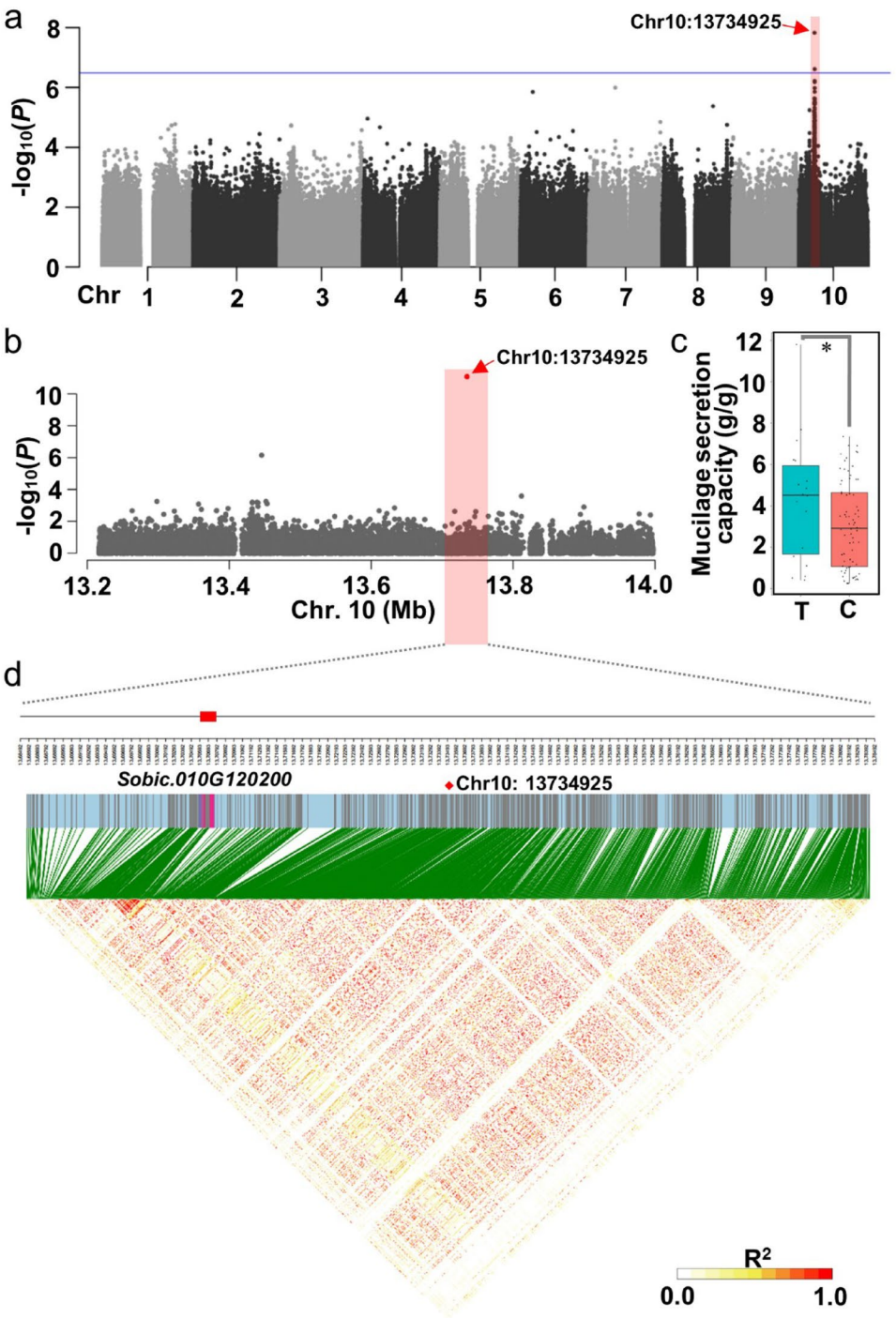

Fig. 6 Genome-wide association study (GWAS) for mucilage secretion capacity in sorghum. **a** Manhattan plot of the GWAS analysis for mucilage secretion capacity by FarmCPU model. The red arrow shows the most significant SNP. **b** Association analysis with SNPs and INDELs in the Significantly Associate Loci (SAL) identified by GWAS. **c** Significance statistics of significant SNPs (T-allele and C-allele) to the phenotypic trait of mucilage secretion capacity, * indicates $P < 0.05$ with (two-tailed) t-test. **d** LD block showing pairwise $r.^2$ values amongst all SNPs in a segment including ~ 50 kb upstream and ~ 50 kb downstream of the significant SNP, red diamonds indicates significant SNP Chr10:13734925

greater mucilage secretion capacity of aerial roots and the longer greening time of leaves in sweet sorghum.

Sierra Mixe maize can secrete a lot of mucilage under sufficient water (Bennett et al. 2020; Van Deynze et al. 2018), Similarly, sorghum aerial roots secret mucilage under rainfall, water spraying, and water immersion, and when the weather is sunny, it stopped secreting mucilage (Figs. 1, 2), which illustrating the close relationship between mucilage and moisture conditions. It has been reported that root exudation can change the capacity of water-retaining properties in the rhizosphere, and the mucilage component in the root exudates is a gel that can absorb a lot of water. In the saturated state, the moisture content in mucilage is 300 times its dry weight, mucilage may be a reservoir that can be absorbed by the roots when the soil is dry (Carminati et al. 2016; Mccully and Boyer 1997). Cryo-scanning electron microscopy revealed a dense three-dimensional matrix that showed a

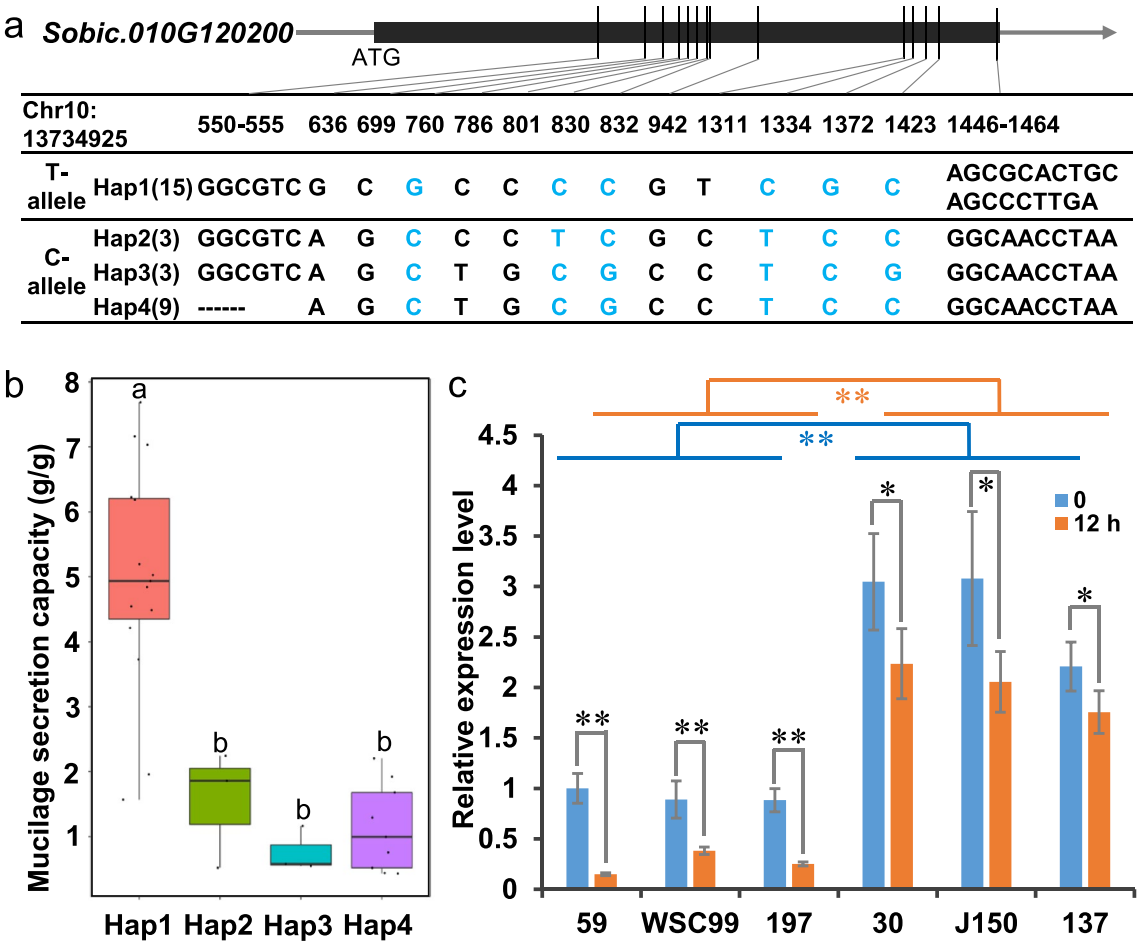

Fig. 7 Haplotype and expression analysis of *Sobic.010G120200*. **a** Haplotypes of *Sobic.010G120200* among two alleles in 30 sorghum accessions (15 accessions in T-allele with higher mucilage secretion capacity and 15 accessions in C-allele with lower mucilage secretion capacity). Four major haplotypes of *Sobic.010G120200* constructed with 14 tag SNPs with a significant difference ($P < 0.05$ with (two-tailed) t-test), and six SNPs caused non-synonymous variation were marked in blue font, and InDel550-555, InDel1446-1464 caused insertion or deletion of two amino acids and Multiple Nucleotide Polymorphism (MNP), respectively. Black box indicates the exon of *Sobic.010G120200*. **b** The mucilage secretion capacity distribution of four haplotypes is displayed by the box plot. In box plots, center values are averages, lines indicate variability outside the upper and lower quartiles, letters indicate a significant difference ($P < 0.05$) using Tukey–Kramer test. **c** The Real-Time Quantitative Reverse Transcription PCR (qRT-PCR) of *Sobic.010G120200* in the aerial roots of three T-allele accessions (59, WSC99, 197) and three C-allele accessions (30, J150, 137) after 12-h water immersion (0-h indicates before water immersion). Expression levels were shown as means ± standard deviation (SD) with four technical replicates; ** indicates $P < 0.01$ and * indicates $P < 0.05$ with (two-tailed) t-test, the blue and orange * represent comparisons between two alleles accessions at 0-h and 12-h, respectively; black * represent comparisons between 0-h and 12-h in single accession

porous network structure possessing interconnected nano and micron pore sizes (Fig. 3a, b). In the natural state of mucilage, water molecules might be confined in the dense three-dimensional network structures which were tightly assembled by the cross-linking, semisolid, and gel-like nanofibers. The structure was similar to sundew adhesive in its predecessors: a dense three-dimensional network structures complex with a large number of water molecules, forming a substance similar to natural hydrogels (Aston et al. 2016; Gorb et al. 2007; Huang et al. 2015). The three-dimensional network microstructure could complex a large number of water molecules, which further verified that moisture is an indispensable factor for mucilage production.

Sierra Mixe maize mucilage is rich in arabinose, fucose, galactose, and polysaccharides, and the underground root exudate in maize also contains arabinose, fucose, and polysaccharides, additionally contains glucose, and xylose (Chaboud 1983; Osborn et al. 1999; Van Deynze et al. 2018). However, we found that the sugar profile of mucilage in sorghum contained high levels of glucose and fructose, while low levels of fucose, arabinose, galactose, xylose, mannose, ribose, galacturonic acid, glucuronic acid, and sucrose (Fig. 3c, d). In addition, the metabolic pathway of

polysaccharides may be involved in the regulation of mucilage secretion (Fig. 4d). The mucilage secretion in sorghum is regulated by glycosyltransferase and glucuronidation-related gene sets through aerial root transcriptomes (Fig. 4, Tables S1–S4). The mucilage secreted by the attachment organs of English ivy (*Hedera helix*), tendrils of Virginia creeper (*Parthenocissus quinquefolia*), abnormal leaves of carnivorous plant Sundew (*Drosera spp*.), epidermal cells of *Arabidopsis thaliana* seed coat, all contain glycoaldehyde acidified compounds (Adlassnig et al. 2010; Bowling and Vaughn 2008; Erni et al. 2011; Huang et al. 2016; Lenaghan and Zhang 2012; Macquet et al. 2007). The main enzyme galacturonosyltransferases coding genes such as *GAUT11*, *GATL5,* and *MUCI70* have been shown to be associated with the mucilage secretion of the *Arabidopsis* seed coat (Arsovski et al. 2010; Caffall et al. 2009; Kong et al. 2013; Tsai et al. 2017; Voiniciuc et al. 2018a). In addition, a non-classified glycosyltransferase *GT106* is probably responsible for the synthesis of the seed coat mucilage (Takenaka et al. 2018). These previous studies in other plants provide support for the involvement of glycosyltransferase and glucuronidation-related genes in sorghum mucilage secretion. The candidate gene *Sobic.010G120200* identified by GWAS belongs to the glycosyltransferase-related gene sets discovered by the transcriptome (Figs. 4, 6), which may control the phenotypic trait of mucilage secretion. By analyzing the haplotypes and expression differences between two alleles accessions, we speculated that this gene may regulate mucilage secretion through a negative regulatory mechanism (Fig. 7). The *Zm00001eb280950* is the orthologous gene of *Sobic.010G120200* in maize (Fig. S5). Genetic transformation can be carried out in maize in the future gene functional research.

The present study has several findings, including 1) great genotypic variation in mucilage secretion in sorghum, 2) the correlation of mucilage secretion capacity and leaf stay-greening degree in sweet sorghum, and 3) the identification of the key gene involved in mucilage secreting capacity. These findings, together with the fact-based hypotheses we proposed, provide the basis for further research on the underlying biology, evolutionary advantage, agronomical function, potential support to nitrogen fixation, and breeding utilization of the mucilage secretion capacity of sorghum.

Materials and methods

Plant materials, field trials, and glasshouse growth conditions

A total of 146 sorghum accessions were used in this research (Table S6). Four sorghum accessions were used for detailed physiological, cytological, and transcriptomic characterisation of the aerial root growth and development and the determination of mucilage secretion capacity. Seeds were sown in the field in mid-April each year from 2018 to 2020 and grown for phenotypic investigation in the experimental field at the Xiangshan Molecular Breeding Base of the Institute of Botany, Chinese Academy of Sciences (Beijing, China; N40°, E116°), and harvested generally from September to October, depending on the growth period and maturity of individual lines. The standard agronomical practice was followed for optimum plant growth and development, including irrigation, fertilizer application, and pest controls. Greenhouse experiments were carried out with a controlled temperature of 30/22 °C day/night cycle, 16 h/8 h light/dark cycle. Seeds of Accession 59 (a genetically improved cultivar), Accession SL35 and SL36 (wild sorghum), and maize B73 were planted in 30-L pots filled with nutritional soil in the greenhouse at the Institute of Botany, Chinese Academy of Sciences.

Observation and quantification of mucilage secretion and aerial root formation

Aerial root formation and mucilage secretion were recorded on three nodes from the bottom of three individual plants of each accession. The field observations of mucilage secretion were repeated three times in 2019. Mucilage secretion was observed one hour after rain, and the secretion lasted for at least five hours. To mimic the effect of rain, we used a water pipe with scattered nozzles to experiment with continuous water spraying in the greenhouse, water pipe runoff was controlled to 4 L/min, and coverage was about 4 m^2 and duration was 24 h. Aerial roots of 1–3 cm in length were used. In 2019, mucilage secretion capacity was quantified between 2–5 p.m in late July and August on two consecutive days, and the humidity condition was below 60%. 2-cm aerial root segments were taken for the collection of phenotypic data in GWAS and the quantification of mucilage secretion was obtained from three biological replicates. The aerial root formation is defined when the measured length ≥ 0.1 cm under an interval of 24 h from day-0 to day-1 until day-30. The record of aerial root formation was selected from five biological replicates and two technical replicates for each material.

Cryo-scanning electron microscopy of mucilage

The mucilage secreted by Accession 59 aerial roots was collected after rain in the field with a 10 mL disposable sterile syringe and transferred into a sterile and dry 1.5 mL centrifuge tube for sample pre-processing. A portion of the collected mucilage was then put into the round-hole liquid sample holder using a 200 µL Gilson pipette. The sample holder was quickly frozen and fixed in supercooled liquid nitrogen

slush with a temperature lower than − 140 °C. Under vacuum conditions, the samples were transferred and installed on the cold console in the sample preparation chamber, the mucilage blocks were then subjected to freezing fracture, sublimation etching, and sputtering coating before ultrastructure observation. The instrument of cryo-scanning electron microscopy (Regulus8100 HITACHI, Japan) with Cryo SEM System (PP3010T Quorum, England) was used for ultrastructure observation of mucilage.

Quantification of soluble sugars content in mucilage

The mucilage samples were lyophilized. A 5 mg lyophilized material sample was dissolved into 500 µL pure water and separated by an ion-exchange chromatography column using the ion chromatography system Thermo ICS 5000+ (Thermo Scientific Dionex, United States) for the quantification of soluble sugars. Three technical replicates were tested for each sample which was obtained by mixing three biological replicates of mucilage with equal mass. For quantification of fructose, arabinose, galactose, glucose, xylose, mannose, fructose, ribose, galacturonic acid, and glucuronic acid, a 20 µL of mucilage was injected into a liquid chromatography column (Dionex™ CarboPac™ PA10 250*4.0 mm); for sucrose quantification, a 25 µL of mucilage was injected into a column of Dionex™ CarboPac™ PA20 (250*3.0 mm) and analyzed. According to the qualitative retention time of the chromatographic peak, the external standard method was used to quantitatively analyze the content of various soluble sugars in the sample to be tested. The concentration of samples was calculated based on the peak area of various soluble sugars, using the concentration of the standard product as the abscissa and the peak area of the standard product as the ordinate to draw the graph, according to the mathematical relationship between the concentration of the standard products and their peak area. The soluble sugars content in samples was calculated through (C*V*F)/M, in which, C represents the concentration of the samples to be tested read by the instrument, in µg/L, V represents the final constant volume of the samples, F represents the dilution multiple of the samples, and M represents the mass of the samples.

RNA isolation and qRT-PCR

The genetically improved cultivar sorghum Accession 59 was used for aerial root transcriptomic analysis. RNA was isolated from 5-day-old aerial roots from sorghum 59 grown from nodes, sampled after raining for 12 h (the maximum mucilage secretion has been reached, Fig. S2); 59-non-secretion were isolated from 5-day-old aerial roots grown from nodes under sunny conditions. Each sample to be tested was obtained by mixing three biological replicates of aerial roots with equal mass, and the samples were sufficiently shaken and crushed, then RNA samples were prepared from the powder of the mixed tissue. Total RNA was extracted using a reagent test kit (Huayueyang Biotech, China). Residual DNA was removed by treatment with RNase-free DNase I at 20–30 °C for 5 min. The concentration and purity of the total RNA were determined using a Nanodrop 2000 spectrophotometer (Nanodrop Technologies, United States). The RNA quality was checked using agarose gel electrophoresis. cDNA pools from the total RNA were synthesized using ReverTra Ace qPCR RT Kit (TOYOBO, Japan) for qPCR. The 10 µL reaction volume contained 5 µL 2 × ultraSYBR Mixture (ComWin Biotech, China), 0.2 µL of each primer (10 µM), and 1 µL cDNA. RT-qPCR experiments were performed using a EcoGold-standard qPCR detection system (Illumina, United States). The variation in expression used by qRT-PCR was estimated using three biological replicates and four technical replicates per bioreplicate. The PCR procedure was scheduled as follows: 95 °C for 10 min, then 40 cycles at 95 °C for 10 s, 57 °C for 20 s, and 72 °C for 30 s. A *β-Actin* gene was used as the reference standard and the relative gene expression level was calculated using a real-time PCR system using the $2^{-\Delta\Delta Ct}$ method (Livak and Schmittgen 2001). Primers for the qRT-PCR are shown in Table S3.

Library construction and transcriptome sequencing

Total RNA, 1 µg, was used for cDNA library construction. Oligo (dT) magnetic beads and ployA oligo were used to isolate mRNA from total RNA. Purified mRNA was cleaved into small fragments of about 300 bp using Fragmentation Buffer (Enzymatics, United States). The first-strand cDNAs were synthesized using reverse transcription and six-base random primers, followed by double-strand cDNA synthesis. Then, the double-stranded cDNAs were purified, end-repaired, ligated to adaptors, and further fragmented, 15 cycles were amplified by PCR for library enrichment, 2% agarose gel was used to recover the target bands, and then mixed on the machine, bridge PCR amplification was carried out, and clusters were generated. Finally, they were sequenced on the Illumina sequencing platform (PE library, read length 2 × 150 bp) (Wang et al. 2021; Zhang et al. 2021).

Differentially expressed genes (DEGs) and GO enrichment analysis

The fragments per kilobases per million reads (FPKM) method was performed using the RSEM software (version 1.3.1) for DEGs (Li and Dewey 2011). The DEGs analysis of 59-secretion vs 59-non-secretion was set as P-adjust < 0.001 and $|\log_2 FC| \geq 1$, the up/down difference multiple was 2.0, and the differential analysis software is DEGseq (http://bioconductor.org/ packages/stats/bioc/DEGSeq/), the most

stringent Bonferroni was used for multiple inspection correction methods. Use the software Goatools (https://files.pythonhosted.org/packages/bb/7b/0c76e3511a79879606672e0741095a891dfb98cd63b1530ed8c51d406cda/goatools-0.8.9.tar.gz) to perform GO enrichment analysis of DEGs, which use fisher exact test, and genes were clustered into three categories: molecular function (MF), biological process (BP), and cellular component (CC) (Wang et al. 2021; Zhang et al. 2021). Bonferroni method was used for multiple test correction, and the GO function was regarded as significantly enriched when *P*-adjust was less than 0.05. The analysis was performed using the online platform Majorbio Cloud Platform by www.majorbio.com (Majorbio Bio-pharm Technology, China). Metabolism pathways were analyzed using iPath3.0 (http://pathways.embl.de).

GWAS and candidate gene prediction

GWAS between mucilage secretion capacity (the average value of three individual plants in each accession) and genome variations was conducted with the FarmCPU model embedded in GAPIT3 (Wang and Zhang 2021). All the genes within a Significantly Associate Loci (SAL) interval (LD decay $r^2 > 0.2$) were identified as potential candidate genes. The annotation of candidate genes was obtained from sorghum genome v3.1 in Phytozome v12 (Goodstein et al. 2012). The extent of LD between significant SNP and *Sobic.010G120200* was calculated by Haploview (Barrett et al. 2005), while the LD of 50 kb upstream and 50 kb downstream of the significant SNP was calculated and plotted with LDBlockShow (Dong et al. 2021).

DNA extraction and Sanger sequencing

The extraction of genomic DNA used a modified cetyltrimethylammonium bromide (CTAB) method (Allen et al. 2006). Primers used to amplify the CDS sequences of *Sobic.010G120200* are shown in Table S3. Q5 High-Fidelity DNA Polymerase (New England Biolabs, United States) was used to prevent the possibility of PCR recombination and sequencing errors. Sanger sequencing was performed by Tsingke Biotech (China).

Statistical analysis

Before significance test of difference, the homogeneity of variance for each group was tested using leveneTest in the car R package (Fox and Weisberg 2018). If the variance among groups was equal, Tukey–Kramer test in the agricolae R package (TukeyHSD function) (De Mendiburu 2014) was performed to test the significance of differences among groups. If not, the Kruskal test in the agricolae R package (Kruskal function) (De Mendiburu 2014) was performed. The mucilage secretion at different aerial root lengths, the aerial roots development and the mucilage secretion capacity distribution amongst haplotypes and subpopulations were analyzed using the above method. The relative expression level and mucilage secretion capacity in two alleles were analyzed using t-test (two-tailed). Tables and figures were prepared using Microsoft Excel 2016 and Microsoft PowerPoint 2016.

Phylogeny reconstruction

The sequences of *Sobic.010G120200* and the orthologous genes in five monocotyledonous plants (*Sorghum bicolor*, *Zea mays*, *Saccharum spontaneum*, *Setaria italica*, *Oryza sativa*) were downloaded from PLAZA monocots version 5.0 (https://bioinformatics.psb.ugent.be/plaza/). The phylogenetic tree based on the amino acid sequences were constructed using MEGA 11 software (Tamura et al. 2021) with both maximum likelihood (ML) methods, branch support values were estimated based on 1,000 bootstrap replicates.

Supplementary Information The online version contains supplementary material available at https://doi.org/10.1007/s11103-023-01365-1.

Acknowledgements We thank Dr. LiDong Wang for providing the phenotyping data of stay-green and leaf senescence.

Author contributions HQH, HCJ and SX designed the experiments. SX performed the experiments and analysed phenotypes and transcriptomes. HG, XYW and ZQL contributed to the variation analysis and GWAS. SX drafted the manuscript. NW revised the earlier versions of the manuscript. HCJ, XQL and HQH discussed the results, contributed to result interpretation, and revised the manuscript. All the authors read and approved the manuscript.

Funding This work was supported by the grants from the National Key R&D Program of China (2019YFD1002701) and the Strategic Priority Research Program of the Chinese Academy of Sciences (XDA26050101).

Data availability The RNA-Seq data has been deposited in the Genome Sequence Archive (http://bigd.big.ac.cn/gsa/) in the BIG Data Center at the Beijing Institute of Genomics (BIG), Chinese Academy of Sciences, under accession numbers CRA010681. The data associated with this article are provided as supplemental materials in the paper.

Code availability Software application and codes used are all publicly available.

Declarations

Competing interest All authors did not have any conflict of interest.

Ethical approval Not applicable.

Consent to participate Not applicable.

Consent for publication All the authors have read and approve the manuscript for publication.

References

Adlassnig W, Lendl T, Peroutka M, Lang I (2010) Deadly glue-adhesive traps of carnivorous plants. biological adhesive systems. Springer, Vienna, pp 15–28. https://doi.org/10.1007/978-3-7091-0286-2_2

Allen GC, Flores-Vergara M, Krasynanski S, Kumar S, Thompson W (2006) A modified protocol for rapid DNA isolation from plant tissues using cetyltrimethylammonium bromide. Nat Protoc 1:2320–2325. https://doi.org/10.1038/nprot.2006.384

Arsovski AA, Haughn GW, Western TL (2010) Seed coat mucilage cells of *Arabidopsis thaliana* as a model for plant cell wall research. Plant Signal Behav 5:796–801. https://doi.org/10.4161/psb.5.7.11773

Aston R, Sewell K, Klein T, Lawrie G, Grøndahl L (2016) Evaluation of the impact of freezing preparation techniques on the characterisation of alginate hydrogels by cryo-SEM. Eur Polym J 82:1–15. https://doi.org/10.1016/j.eurpolymj.2016.06.025

Badri DV, Vivanco JM (2009) Regulation and function of root exudates. Plant Cell Environ 32:666–681. https://doi.org/10.1111/j.1365-3040.2009.01926.x

Baetz U, Martinoia E (2014) Root exudates: the hidden part of plant defense. Trends Plant Sci 19:90–98. https://doi.org/10.1016/j.tplants.2013.11.006

Bais HP, Weir TL, Perry LG, Gilroy S, Vivanco JM (2006) The role of root exudates in rhizosphere interactions with plants and other organisms. Annu Rev Plant Biol 7:233–266. https://doi.org/10.1146/annurev.arplant.57.032905.105159

Barrett JC, Fry B, Maller J, Daly MJ (2005) Haploview: analysis and visualization of LD and haplotype maps. Bioinformatics 21:263–265. https://doi.org/10.1093/bioinformatics/bth457

Bennett AB, Pankievicz VCS, Ane J (2020) A model for nitrogen fixation in cereal crops. Trends Plant Sci 25:226–235. https://doi.org/10.1016/j.tplants.2019.12.004

Borrell A, Hammer G, Van Oosterom E (2001) Stay-green: a consequence of the balance between supply and demand for nitrogen during grain filling? Ann Appl Biol 138:91–95. https://doi.org/10.1111/j.1744-7348.2001.tb00088.x

Bowling A, Vaughn K (2008) Structural and immunocytochemical characterization of the adhesive tendril of Virginia creeper (*Parthenocissus quinquefolia* [L.] Planch.). Protoplasma 232:153. https://doi.org/10.1007/s00709-008-0287-x

Brenton Z, Cooper EA, Myers MT, Boyles RE, Shakoor N, Zielinski KJ, Rauh BL, Bridges WC, Morris GP, Kresovich S (2016) A genomic resource for the development, improvement, and exploitation of sorghum for bioenergy. Genetics 204:21–33. https://doi.org/10.1534/genetics.115.183947

Brown LK, George TS, Neugebauer K, White PJ (2017) The rhizosheath-a potential trait for future agricultural sustainability occurs in orders throughout the angiosperms. Plant Soil 418:115–128. https://doi.org/10.1007/s11104-017-3220-2

Bulgarelli D, Schlaeppi K, Spaepen S, Van Themaat EVL, Schulze-Lefert P (2013) Structure and functions of the bacterial microbiota of plants. Annu Rev Plant Biol 64:807–838. https://doi.org/10.1146/annurev-arplant-050312-120106

Caffall KH, Pattathil S, Phillips SE, Hahn MG, Mohnen D (2009) *Arabidopsis thaliana* T-DNA mutants implicate *GAUT* genes in the biosynthesis of pectin and xylan in cell walls and seed testa. Mol Plant 2:1000–1014. https://doi.org/10.1093/mp/ssp062

Carminati A (2012) A model of root water uptake coupled with rhizosphere dynamics. Vadose Zone J 11:vzj2011.0106. https://doi.org/10.2136/vzj2011.0106

Carminati A, Zarebanadkouki M, Kroener E, Ahmed MA, Holz M (2016) Biophysical rhizosphere processes affecting root water uptake. Ann Bot 118:561–571. https://doi.org/10.1093/aob/mcw113

Chaboud A (1983) Isolation, purification and chemical composition of maize root cap slime. Plant Soil 73:395–402. https://doi.org/10.1007/BF02184316

Czarnes S, Dexter AR, Bartoli F (2000a) Wetting and drying cycles in the maize rhizosphere under controlled conditions. Mechanics of the root-adhering soil. Plant Soil 221:253–271. https://doi.org/10.1023/A:1004747323220

Czarnes S, Hallett PD, Bengough AG, Young IM (2000b) Root-and microbial-derived mucilages affect soil structure and water transport. Eur J Soil Sci 51:435–443. https://doi.org/10.1046/j.1365-2389.2000.00327.x

De Mendiburu F (2014) Agricolae: statistical procedures for agricultural research. R Package Version 1:1–4

Dong SS, He WM, Ji JJ, Zhang C, Guo Y, Yang TL (2021) LDBlockShow: a fast and convenient tool for visualizing linkage disequilibrium and haplotype blocks based on variant call format files. Brief Bioinform 22:bbaa227. https://doi.org/10.1093/bib/bbaa227

Erni P, Varagnat M, Clasen C, Crest J, McKinley GH (2011) Microrheometry of sub-nanolitre biopolymer samples: non-Newtonian flow phenomena of carnivorous plant mucilage. Soft Matter 7:10889–10898. https://doi.org/10.1039/C1SM05815K

Fox J, Weisberg S (2018) An R companion to applied regression. Sage Publications

Galloway AF, Knox P, Krause K (2020) Sticky mucilages and exudates of plants: putative microenvironmental design elements with biotechnological value. New Phytol 225:1461–1469. https://doi.org/10.1111/nph.16144

Gaume L, Forterre Y (2007) A viscoelastic deadly fluid in carnivorous pitcher plants. PLoS ONE 2:e1185. https://doi.org/10.1371/journal.pone.0001185

Goodstein DM, Shu S, Howson R, Neupane R, Hayes RD, Fazo J, Mitros T, Dirks W, Hellsten U, Putnam N (2012) Phytozome: a comparative platform for green plant genomics. Nucl Acids Res 40:D1178–D1186. https://doi.org/10.1093/nar/gkr944

Gorb S, Voigt D, Gorb E (2007) Visualisation of small fluid droplets on biological and artificial surfaces using the cryo-SEM approach. Mod Res Edu Topic Microsc 2:812–819

Groot EP, Sweeney EJ, Rost TL (2003) Development of the adhesive pad on climbing fig (*Ficus pumila*) stems from clusters of adventitious roots. Plant Soil 248:85–96. https://doi.org/10.1023/A:1022342025447

Haughn GW, Western TL (2012) *Arabidopsis* seed coat mucilage is a specialized cell wall that can be used as a model for genetic analysis of plant cell wall structure and function. Front Plant Sci 3:64. https://doi.org/10.3389/fpls.2012.00064

Higdon SM, Pozzo T, Tibbett EJ, Chiu C, Jeannotte R, Weimer BC, Bennett AB (2020) Diazotrophic bacteria from maize exhibit multifaceted plant growth promotion traits in multiple hosts. PLoS One 15:e0239081. https://doi.org/10.1371/journal.pone.0239081

Huang Z, Gutterman Y, Osborne DJ (2004) Value of the mucilaginous pellicle to seeds of the sand-stabilizing desert woody shrub *Artemisia sphaerocephala* (Asteraceae). Trees 18:669–676. https://doi.org/10.1007/s00468-004-0349-4

Huang Y, Wang Y, Sun L, Agrawal R, Zhang M (2015) Sundew adhesive: a naturally occurring hydrogel. J R Soc Interface 12:20150226. https://doi.org/10.1098/rsif.2015.0226

Huang Y, Wang Y, Tan L, Sun L, Petrosino J, Cui M-Z, Hao F, Zhang M (2016) Nanospherical arabinogalactan proteins are a key component of the high-strength adhesive secreted by English ivy. Proc Natl Acad Sci USA 113:E3193–E3202. https://doi.org/10.1073/pnas.1600406113

Kong Y, Zhou G, Abdeen AA, Schafhauser J, Richardson B, Atmodjo MA, Jung J, Wicker L, Mohnen D, Western T (2013) GALACTURONOSYLTRANSFERASE-LIKE5 is involved in the production of *Arabidopsis* seed coat mucilage. Plant Physiol 163:1203–1217. https://doi.org/10.1104/pp.113.227041

Lenaghan SC, Zhang M (2012) Real-time observation of the secretion of a nanocomposite adhesive from English ivy (*Hedera helix*). Plant Sci 183:206–211. https://doi.org/10.1016/j.plantsci.2011.08.013

Li B, Dewey CN (2011) RSEM: accurate transcript quantification from RNA-Seq data with or without a reference genome. BMC Bioinform 12:1–16. https://doi.org/10.1186/1471-2105-12-323

Li G, Zhang ZS, Gao HY, Liu P, Dong ST, Zhang JW, Zhao B (2012) Effects of nitrogen on photosynthetic characteristics of leaves from two different stay-green corn (*Zea mays* L.) varieties at the grain-filling stage. Can J Plant Sci 92:671–680. https://doi.org/10.4141/cjps2012-039

Livak KJ, Schmittgen TD (2001) Analysis of relative gene expression data using real-time quantitative PCR and the $2^{-\Delta\Delta CT}$ method. Methods 25:402–408. https://doi.org/10.1006/meth.2001.1262

Mace ES, Tai S, Gilding EK, Li Y, Prentis PJ, Bian L, Campbell BC, Hu W, Innes DJ, Han X (2013) Whole-genome sequencing reveals untapped genetic potential in Africa's indigenous cereal crop sorghum. Nat Commun 4:2320. https://doi.org/10.1038/ncomms3320

Macquet A, Ralet M-C, Kronenberger J, Marion-Poll A, North HM (2007) In situ, chemical and macromolecular study of the composition of *Arabidopsis thaliana* seed coat mucilage. Plant Cell Physiol 48:984–999. https://doi.org/10.1093/pcp/pcm068

Mccully ME, Boyer JS (1997) The expansion of maize root-cap mucilage during hydration. 3. Changes in water potential and water content. Physiol Plant 99:169–177. https://doi.org/10.1111/j.1399-3054.1997.tb03445.x

Melzer B, Steinbrecher T, Seidel R, Kraft O, Schwaiger R, Speck T (2010) The attachment strategy of English ivy: a complex mechanism acting on several hierarchical levels. J R Soc Interface 7:1383–1389. https://doi.org/10.1098/rsif.2010.0140

Narasimhan K, Basheer C, Bajic VB, Swarup S (2003) Enhancement of plant-microbe interactions using a rhizosphere metabolomics-driven approach and its application in the removal of polychlorinated biphenyls. Plant Physiol 132:146–153. https://doi.org/10.1104/pp.102.016295

Osborn HMI, Lochey F, Mosley L, Read DB (1999) Analysis of polysaccharides and monosaccharides in the root mucilage of maize (*Zea mays* L.) by gas chromatography. J Chromatogr 831:267–276. https://doi.org/10.1016/S0021-9673(98)00935-2

Read DB, Gregory PJ (1997) Surface tension and viscosity of axenic maize and lupin root mucilages. New Phytol 137:623–628. https://doi.org/10.1046/j.1469-8137.1997.00859.x

Read DB, Bengough AG, Gregory PJ, Crawford JW, Robinson D, Scrimgeour CM, Young IM, Zhang K, Zhang X (2003) Plant roots release phospholipid surfactants that modify the physical and chemical properties of soil. New Phytol 157:315–326. https://doi.org/10.1046/j.1469-8137.2003.00665.x

Rooney WL, Blumenthal JM, Bean B, Mullet JE (2007) Designing sorghum as a dedicated bioenergy feedstock. Biofuels Bioprod Biorefin 1:147–157. https://doi.org/10.1002/bbb.15

Sasse J, Martinoia E, Northen T (2018) Feed your friends: do plant exudates shape the root microbiome? Trends Plant Sci 23:25–41. https://doi.org/10.1016/j.tplants.2017.09.003

Sechet J, Marion-Poll A, North HM (2018) Emerging functions for cell wall polysaccharides accumulated during eudicot seed development. Plants 7(4):81. https://doi.org/10.3390/plants7040081

Sigida EN, Fedonenko YP, Shashkov AS, Zdorovenko EL, Konnova SA, Ignatov VV, Knirel YA (2013) Structural studies of the O-specific polysaccharide(s) from the lipopolysaccharide of *Azospirillum brasilense* type strain Sp7. Carbohydr Res 380:76–80. https://doi.org/10.1016/j.carres.2013.07.013

Takenaka Y, Kato K, Ogawa-Ohnishi M, Tsuruhama K, Kajiura H, Yagyu K, Takeda A, Takeda Y, Kunieda T, Hara-Nishimura I (2018) Pectin RG-I rhamnosyltransferases represent a novel plant-specific glycosyltransferase family. Nat Plants 4:669–676. https://doi.org/10.1038/s41477-018-0217-7

Tamura K, Stecher G, Kumar S (2021) MEGA11: molecular evolutionary genetics analysis version 11. Mol Biol Evol 38:3022–3027. https://doi.org/10.1093/molbev/msab120

Tsai AY-L, Kunieda T, Rogalski J, Foster LJ, Ellis BE, Haughn GW (2017) Identification and characterization of *Arabidopsis* seed coat mucilage proteins. Plant Physiol 173:1059–1074. https://doi.org/10.1104/pp.16.01600

Van Deynze A, Zamora P, Delaux P-M, Heitmann C, Jayaraman D, Rajasekar S, Graham D, Maeda J, Gibson D, Schwartz KD (2018) Nitrogen fixation in a landrace of maize is supported by a mucilage-associated diazotrophic microbiota. PLoS Biol 16:e2006352. https://doi.org/10.1371/journal.pbio.2006352

Van Oosterom E, Chapman S, Borrell A, Broad IJ, Hammer G (2010) Functional dynamics of the nitrogen balance of sorghum. II. Grain filling period. Field Crops Res 115:29–38. https://doi.org/10.1016/j.fcr.2009.09.019

Voiniciuc C, Engle KA, Günl M, Dieluweit S, Schmidt MHW, Yang JY, Moremen KW, Mohnen D, Usadel B (2018a) Identification of key enzymes for pectin synthesis in seed mucilage. Plant Physiol 178:1045–1064. https://doi.org/10.1104/pp.18.00584

Voiniciuc C, Pauly M, Usadel B (2018b) Monitoring polysaccharide dynamics in the plant cell wall. Plant Physiol 176:2590–2600. https://doi.org/10.1104/pp.17.01776

Wang J, Zhang Z (2021) GAPIT Version 3. boosting power and accuracy for genomic association and prediction. Genom Proteom Bioinf 19:629–640. https://doi.org/10.1016/j.gpb.2021.08.005

Wang C, Chen L, Cai Z, Chen C, Liu Z, Liu S, Zou L, Tan M, Chen J, Liu X (2021) Metabolite profiling and transcriptome analysis explains difference in accumulation of bioactive constituents in licorice (*Glycyrrhiza uralensis*) under salt stress. Front Plant Sci 12:727882. https://doi.org/10.3389/fpls.2021.727882

Wani S (1986) Cereal nitrogen fixation: proceedings of the Working Group Meeting held at ICRISAT Center, India, 9–12 October 1984. International Crops Research Institute for the Semi-Arid Tropics

Wu X, Liu Y, Luo H, Shang L, Leng C, Liu Z, Li Z, Lu X, Cai H, Hao H (2022) Genomic footprints of sorghum domestication and breeding selection for multiple end uses. Mol Plant 15:537–551. https://doi.org/10.1016/j.molp.2022.01.002

Zhalnina K, Louie KB, Hao Z, Mansoori N, da Rocha UN, Shi S, Cho H, Karaoz U, Loqué D, Bowen BP (2018) Dynamic root exudate chemistry and microbial substrate preferences drive patterns in rhizosphere microbial community assembly. Nat Microbiol 3:470–480. https://doi.org/10.1038/s41564-018-0129-3

Zhang G, Tang R, Niu S, Si H, Yang Q, Rajora OP, Li XQ (2021) Heat-stress-induced sprouting and differential gene expression in growing potato tubers: comparative transcriptomics with that induced by postharvest sprouting. Hortic Res 8:1–18. https://doi.org/10.1038/s41438-021-00680-2

Zheng LY, Guo XS, He B, Sun LJ, Peng Y, Dong SS, Liu TF, Jiang S, Ramachandran S, Liu CM (2011) Genome-wide patterns of genetic variation in sweet and grain sorghum (*Sorghum bicolor*). Genome Biol 12:1–15. https://doi.org/10.1186/gb-2011-12-11-r114

Zhu Z, Li D, Cong L, Lu X (2021) Identification of microRNAs involved in crosstalk between nitrogen, phosphorus and potassium under multiple nutrient deficiency in sorghum. Crop J 9:465–475. https://doi.org/10.1016/j.cj.2020.07.005